Journal of Molecular Neuroscience

Biochemical characterization of a caspase-3 far red fluorescent probe for non-invasive optical imaging of neuronal apoptosis

--Manuscript Draft--

Manuscript Number:	
Full Title:	Biochemical characterization of a caspase-3 far red fluorescent probe for non-invasive optical imaging of neuronal apoptosis
Article Type:	SI: Peptides
Keywords:	Apoptosis; caspase-3; stroke; imaging.
Corresponding Author:	valerie jolivel mont-saint-aignan, FRANCE
Corresponding Author Secondary Information:	
Corresponding Author's Institution:	
Corresponding Author's Secondary Institution:	
First Author:	valerie jolivel
First Author Secondary Information:	
Order of Authors:	valerie jolivel
	Sébastien Arthaud
	Béatrice Botia
	Christophe Portal
	Bruno Delest
	Guillaume Clavé
	Jérôme Leprince
	Anthony Romieu
	Pierre-Yves Renard
	Omar Touzani
	Heidi Ligeret
	Pauline Noack
	Marc Massonneau
	Alain Fournier
	Hubert Vaudry
	David Vaudry
Order of Authors Secondary Information:	
Abstract:	Apoptosis is a regulated process, leading to cell death, which is involved in several pathologies including neurodegenerative diseases and stroke. Caspase 3 is a key enzyme of the apoptotic pathway and is considered as a major target for the treatment of abnormal cell death. Sensitive and non-invasive methods to monitor caspase 3 activity in cells and in the brain of living animals are needed to test the efficiency of novel therapeutic strategies. In the present study, we have biochemically characterized a caspase 3 far red fluorescent probe, QCASP3.2, that can be used to detect apoptosis in vivo. The specificity of cleavage of QCASP3.2 was demonstrated using recombinant caspases and protease inhibitors. The functionality of the probe was also

	established in cerebellar neurons cultured in apoptotic conditions. QCASP3.2 did not exhibit any toxicity and appeared to accurately reflect the induction and inhibition of caspase activity by H2O2 and PACAP, respectively, both in cell lysates and in cultured neurons. Finally, intravenous injection of the probe after cerebral ischemia revealed activation of caspase 3 in the infarcted hemisphere. Thus the present study demonstrates that QCASP3.2 is a suitable probe to monitor apoptosis both in vitro and in vivo, and illustrates some of the possible applications of this caspase 3 fluorescent probe.

Biochemical characterization of a caspase-3 far red fluorescent probe for non-invasive optical imaging of neuronal apoptosis

Valérie Jolivel,[a,b,c,d] Sébastien Arthaud,[e] Béatrice Botia,[a,b,d] Christophe Portal,[c,f] Bruno Delest,[c] Guillaume Clavé,[c,f] Jérôme Leprince,[a,b,d,e] Anthony Romieu,[f,g] Pierre-Yves Renard,[f,g] Omar Touzani,[h] Heidi Ligeret,[c] Pauline Noack,[c] Marc Massonneau,[c] Alain Fournier,[d,i] Hubert Vaudry,[a,b,d,e] AND David Vaudry[a,b,d,e*]

[a] *European Institute for Peptide Research (IFRMP23), University of Rouen, 76821 Mont-Saint-Aignan, France*

[b] *INSERM U982, DC2N, 76821 Mont-Saint-Aignan, France*

[c] *QUIDD, Pharmaparc II, Voie de l'Innovation, 27100, Val de Reuil, France*

[d] *International Associated Laboratory Samuel de Champlain, University of Rouen, 76821 Mont-Saint-Aignan, France and University of Québec, Laval, H7V 1B7, Canada*

[e] *Cell Imaging Platform of Normandy (PRIMACEN), University of Rouen, 76821 Mont-Saint-Aignan, France*

[f] *Equipe de chimie Bio-Organique, IFRMP23, COBRA CNRS UMR 6014 & FR 3038, IRCOF, 76131 Mont-Saint-Aignan, France*

[g] *University of Rouen, IRCOF, rue Tesnière, 76821 Mont-Saint-Aignan, France*

[h] *Cervoxy team, CNRS UMR 6232, Cycéron, 14074 Caen, France*

[i] *Institut National de la Recherche Scientifique–Institut Armand-Frappier, University of Québec, Pointe Claire, Laval H7V1B7, Canada*

* Corresponding author.

Mailing address: INSERM U982, University of Rouen, 76821 Mont-Saint-Aignan, France. E-mail: david.vaudry@univ-rouen.fr Tel: +33 2 35 14 67 60; Fax: +33 2 35 14 69 46.

Abstract

Apoptosis is a regulated process, leading to cell death, which is involved in several pathologies including neurodegenerative diseases and stroke. Caspase-3 is a key enzyme of the apoptotic pathway and is considered as a major target for the treatment of abnormal cell death. Sensitive and non-invasive methods to monitor caspase-3 activity in cells and in the brain of living animals are needed to test the efficiency of novel therapeutic strategies. In the present study, we have biochemically characterized a caspase-3 far red fluorescent probe, QCASP3.2, that can be used to detect apoptosis *in vivo*. The specificity of cleavage of QCASP3.2 was demonstrated using recombinant caspases and protease inhibitors. The functionality of the probe was also established in cerebellar neurons cultured in apoptotic conditions. QCASP3.2 did not exhibit any toxicity and appeared to accurately reflect the induction and inhibition of caspase activity by H_2O_2 and PACAP, respectively, both in cell lysates and in cultured neurons. Finally, intravenous injection of the probe after cerebral ischemia revealed activation of caspase-3 in the infarcted hemisphere. Thus the present study demonstrates that QCASP3.2 is a suitable probe to monitor apoptosis both *in vitro* and *in vivo*, and illustrates some of the possible applications of this caspase-3 fluorescent probe.

Keywords

Apoptosis; caspase-3; stroke; imaging.

Introduction

Cerebrovascular accidents represent the third cause of death in industrialized countries just after cardiovascular diseases and cancers. In 87% of the cases, these accidents are due to occlusion of a cerebral artery which causes abrupt deprivation of oxygen and consequently provokes massive neuronal cell death in a brain area (Lloyd-Jones et al. 2009). After ischemia, cells located at the centre of the lesion die by necrosis while, in the peripheral zone, cells degenerate through an apoptotic process (Zheng et al. 2003).

Apoptosis is a universal programmed cell death mechanism that plays a pivotal role in normal development and homeostasis (Jacobson et al. 1997). Dysregulation of apoptosis is involved in various pathologies such as cancers, neurodegenerative diseases and stroke. Apoptosis is characterized by a series of cellular events including cytoplasm shrinkage, DNA fragmentation and membrane blebbing (Elmore 2007). At the molecular level, these morphological changes have been ascribed to a complex cascade of biochemical pathways leading to the activation of specific and highly conserved proteases, the caspases (**c**ysteine-dependent **asp**artate specific prote**ase**; (Alnemri et al. 1996)).

The term caspase designates a family of proteases that are synthesized as inactive zymogens and get activated through proteolytic cleavage at specific internal aspartate residues (Liu et al. 2005). Active caspases are heterotetramers composed of two large and two short subunits (Rotonda et al. 1996). Most caspases are involved in apoptosis and can be divided into two subfamilies. The first group includes the initiator caspases (caspase-2, -8, -9 and -10) which exhibit an N-terminal adapter domain involved in the auto-cleavage process, while the second group corresponds to the effector caspases (caspase-3, -6 and -7) which lack the N-terminal adapter domain and get activated by initiator caspases. Each caspase recognizes a specific sequence, generally composed

of four amino acids, and cleaves at the C-terminus of the last aspartate residue (Hengartner 2000). Activation of caspases initiates a series of events that ultimately lead to morphological alterations characteristic of the apoptotic cell death.

Caspase-3 (EC 3.4.22.56) is considered as a key effector enzyme of the apoptotic cascade (Lakhani et al. 2006), is involved in neuronal cell death *in vitro,* following exposure to toxic molecules (Vaudry et al. 2002; Takadera et al. 2007), and *in vivo,* after for instance cerebral ischemia (Love et al. 2000; Zhu et al. 2004). Characterization of the natural target of caspase-3 has revealed that this enzyme has a high specificity of cleavage for the tetrapeptide Asp-Glu-Val-Asp (DEVD; (Stennicke and Salvesen 1997)).

In vivo molecular imaging is based on three major technologies making use of either contrast agents (magnetic resonance imaging), radio-emitting isotopes (positron emission tomography) or light emitting species (optical imaging). Among these technologies, optical imaging presents the advantages of being rapid, inexpensive and safe. Therefore, optical imaging is emerging as a powerful diagnostic/prognostic approach for the detection of various diseases such as cancer (Weissleder and Pittet 2008), inflammation (Cortez-Retamozo et al. 2008) or degenerative disorders (Raymond et al. 2008). Nevertheless, this technique exhibits some constraints such as the choice of the excitation and emission wavelengths which have to be in the near-infrared domain where the absorption by tissues is minimum (Weissleder and Ntziachristos 2003).

Non-invasive optical imaging of apoptosis has initially been carried out with fluorochrome-labeled annexin-5 which specifically targets phosphatidylserine moieties that are externalized when cells enter into apoptosis (Petrovsky et al. 2003). However, these probes have major limitations since they are unable to distinct apoptotic from necrotic cells, inasmuch as they penetrate into permeabilized necrotic cells and subsequently bind to phosphatidylserines that are

at the internal side of the cell membrane. More recently, other probes have been developed that directly target caspase-3 and become fluorescent only in the presence of active caspase-3, thus substantially increasing signal specificity (Bullok and Piwnica-Worms 2005; Lapeyre et al. 2006). Functionality of these probes was demonstrated in human colon xenografts and in liver abscess mouse models (Bullok et al. 2007), in isolated heart reperfusion injury (Pantos et al. 2009) or after intra-dermal injection of caspase-3 (Zhang et al. 2009).

In this context, the aim of the present study was to characterize a fluorescent probe targeting caspase-3, and to validate the suitability of the probe by investigating the efficiency of protective molecules in *in vitro* and *in vivo* models of neuronal cell death.

Material and methods

Chemicals and reagents

Recombinant human caspase-3 was purchased from Sigma (Saint-Quentin Fallavier, France), murine caspases-1, -3 and -8 were from Biovision (Mountain View, CA, USA) and murine caspase-11 was from Biomol (Plymouth Meeting, PA, USA). Antipain, leupeptin, Z-VAD-FMK, Ac-YVAD-CHO, Ac-DEVD-CHO, fluorescein diacetate, H_2O_2 and all culture reagents were from Sigma. Multiwell plates and petri dishes were from Costar (Cambridge, MA, USA). Calcein was from Molecular Probe (Cergy Pontoise, France) and the Apo-ONE™ Homogeneous Caspase-3/7 Assay kit was from Promega (Charbonnières, France).

PACAP38 was synthesized using the fluorenylmethyloxycarbonyl (Fmoc) chemistry methodology using a semi-automatic multireactor system. A rink-amide resin was used as a solid support and amino acids were introduced under their Fmoc-N-protected form. Couplings were performed in N,N-dimethylformamide in the presence of diisopropylethylamine using benzotriazol-1-yl-oxy-trishexafluorophosphate as a coupling reagent. N-terminal deprotection was achieved with 40% piperidine in DMF, and PACAP38 was cleaved from the solid support using trifluoroacetic acid (TFA) containing ethanedithiol, phenol and water as scavengers. After evaporation of TFA, the remaining material was precipitated. Crude PACAP38, dissolved in aqueous TFA (0.06%), was purified by HPLC and the molecular weight of the peptide was verified by MALDI-TOF mass spectrometry.

Three probes were used for the study: QCASP3.2; a control probe corresponding to QCASP3.2 in which the L-Val was replaced by the antipodal D-Ala; and a probe corresponding to cleaved QCASP3.2.

In vitro characterization of QCASP3.2

For the determination of biochemical values, QCASP3.2 was diluted in caspase-3 buffer (100 mM NaCl, 40 mM HEPES, 10 mM DTT, 1 mM EDTA, 10% (w/v) sucrose and 0.1% (w/v) CHAPS, pH 7.4) in the presence of 10% DMSO, which has previously been reported not to affect caspase activity (Kume et al. 2006), at concentrations ranging from 0.125 to 16 µM. Each dilution of QCASP3.2 was then incubated with 20 nM of caspase-3 at 37°C for 2 hours and recorded every 30 seconds on a FlexStation II microplate reader (Molecular Devices Corporation, Sunnydale, CA, USA; $\lambda_{excitation}$ = 645 nm, $\lambda_{emission}$ = 670 nm, cut-off filter = 665

nm). A standard curve using the probe equivalent to cleaved QCASP3.2 was used to convert fluorescence units into moles of formed product. The inner-filter effect was corrected as previously described (Liu et al. 1999). The V_i was measured for each substrate concentration and K_M, V_{max}, k_{cat} and k_{cat}/K_M values were determined by means of the double-inverse relation of Lineweaver-Burk.

Recombinant human caspase-3, murine caspases-1, -3, -8 and -11 or 10 µL of mouse plasma were incubated in caspase buffer for 75 minutes at 37°C to determine QCASP3.2 specificity. The final concentration of each caspase was adjusted to obtain a volumic activity of 0.5 pmol/min/µL per well. QCASP3.2 was then added (1 µM) and the kinetics of cleavage in each condition was monitored at 37°C for 5 hours on the microplate reader. In some wells, 0.25 µM of the caspase-3 inhibitor Ac-DEVD-CHO was added 1 hour prior to QCASP3.2.

Animals

Wistar rats were obtained from Charles River Laboratories (L'Arbresle, France) and C57BL/6 mice from Janvier (Le Genest Saint-Isle, France). Animals were kept in a temperature-controlled environment (21 ± 1ºC) under an established photoperiod (lights on 07.00-19.00 h) with free access to food and tap water. Animal procedures were performed under the supervision of authorized investigators in accordance with the European Union normative for care and use of experimental animals.

Cell culture, treatments and *in cellulo* investigations

Primary cerebellar granule cells (CGC) were isolated from cerebella of 8-day-old Wistar rats and cultured as previously described (Gonzalez et al. 1997; Vaudry et al. 2002). Neurons were treated, 24 hours after plating, with medium, H_2O_2 (10 to 160 µM) and/or PACAP (100 nM). To investigate caspase activity, 6 hours after treatment, cells seeded in 35-mm-diameter dishes (300,000 cells/cm^2) were scratched and incubated with the Apo-ONE Caspase-3/7 Assay kit. Fluorescence intensity was measured over a 3-hour period with the microplate reader ($\lambda_{excitation}$ = 485 nm, $\lambda_{emission}$ = 530 nm). For cell survival experiments, 24 hours after treatment, cells seeded in 24-multiwell plates were incubated with fluorescein diacetate as previously described (Vaudry et al. 2002).

To investigate QCASP3.2 cleavage, 6 hours after treatment, cells seeded in 35-mm-diameter dishes were scratched and diluted in caspase-3 buffer in the presence of QCASP3.2 (1 µM). Fluorescence was then measured with the microplate reader and, for each condition, V_i was determined after subtracting QCASP3.2 background fluorescence observed in the absence of cells. To evaluate QCASP3.2 cleavage in living neurons, cells were seeded in 96-multiwell plates. Six hours after treatment, QCASP3.2 (5 µM) was added and fluorescence intensity was measured to calculate in each well the V_i. To establish whether QCASP3.2 was cleaved into cells or not, the probe was also incubated with cell culture supernatants.

To assess QCASP3.2 specificity, 6 hours after induction of apoptosis by H_2O_2, cells seeded in 24-multiwell plates were scratched and incubated in 96-well plates with caspase-3 buffer in the presence of graded concentrations of inhibitors (10 pM to 10 µM). After 15 minutes at 37°C, QCASP3.2 (1 µM) was added in each well and the fluorescence intensity was measured over a 3-hour period to determine for each inhibitor the V_i and the IC_{50} values. The K_i were also calculated by means of the Cheng-Pruschoff relation with [S] = 1 µM.

For confocal microscopy and flow cytometry analysis, cells were seeded at densities of 187,000 and 375,000 cells/cm^2, respectively. Six hours after treatment, cells were incubated with 1.2 µM calcein and 4 µM QCASP3.2 for 30 minutes at 37°C. Neurons were then washed with PBS and either directly observed by confocal microscopy (SP2, Leica) or detached with 500 µL PBS-EDTA for flow cytometry analysis (FACScalibur, Becton Dickinson).

In vivo investigations

Four-month-old male C57BL/6 mice underwent permanent focal cerebral ischemia using the electrocoagulation technique. Briefly, mice were anesthetized by an intraperitoneal injection of ketamine (l00 mg/kg, Imalgene) / xylazine (10 mg/kg, Rompun). After shaving the temporal side of the head, a skin incision was made between the eye and the ear. The temporalis muscle was incised and retracted. Then, a hole was made with a microdrill in the skull to perform electrocoagulation of the right middle cerebral artery. After surgery, all animals were placed in a warmed ventilated rack (Charles River Laboratories) maintained at 26°C with a dark/light cycle (light between 07.00 h and 19.00 h). Twenty-four hours after ischemia, animals received an intravenous injection of 2 nmoles of QCASP3.2, and 24 hours later, animals were euthanized. Brains were dissected out, frozen in isopentane cooled at –30°C with dry ice and stored at –80°C until use.

Frozen brains were cut into 60-µm-thick tissue sections mounted on gelatin glass slides and stored at –20°C. For histological analysis, the brain sections were fixed in 4% paraformaldehyde for 20 minutes and stained with acetate thionine. Each section was photographed with a scale bar. The areas of infarction were delineated based on the lack of staining in the ischemic area and

measured by using NIH ImageJ software. Infarct area in each section was determined as: total area of the contralateral hemisphere – (total area of the ischemic hemisphere – infarcted area). The infarct volume was calculated as: ∑ infarct areas over all affected brain slices × distance between two consecutive slices. Infarct volume was further corrected for edema volume as described earlier (Lin et al. 1997). For immunohistochemical analysis, the brain sections were fixed in 4% paraformaldehyde and incubated overnight at 4°C in buffer containing 1% BSA and 3% Triton X-100 with the primary antibody against cleaved caspase-3 (1/200, Cell Signaling). Tissue slices were rinced in PBS and incubated at room temperature for 90 minutes with the secondary antibody. Finally, the slices were mounted with PBS-glycerol (50%/50%). To study in vivo cleavage of QCASP3.2 after cerebral ischemia, the brain sections were fixed for 30 min with 4% paraformaldehyde, rinsed in PBS and mounted with PBS-glycerol (50%/50%) before microscopic observation.

Statistical analysis

All data were analyzed using the PRISM4 software. Data are presented as mean ± SEM from at least three independent experiments performed in triplicate. Statistical analysis of the data was conducted using a non-parametric test (Mann-Withney or Kruskal-Wallis tests) followed by a Dunn's multiple comparison test.

Results

Structure of QCASP3.2 and the control probe

A protease-activable near infra-red fluorescent probe, designated QCASP3.2, was engineered to be sensitive and specific for caspase-3 activity by using the peptide substrate Asp-Glu-Val-Asp (DEVD), flanked by two anchoring aminoacids with an N-acetylcystein at the N-terminal and a lysine-amide at the C-terminal extremity (Fig. 1). The Cy5.0 was grafted at the N-terminal side of the peptide structure and the quenching group QSY®21 at the other side (Fig. 1). The resulting far-red fluorogenic QCASP3.2 probe revealed quenching values of 96.5% and 88.3% in caspase-3 buffer and mouse plasma, respectively (in conditions avoiding inter-molecular quenching phenomenon). The probe exhibited a relatively good solubility in basic aqueous buffers (caspase-3 buffer, PBS or $NaHCO_3$ solution), acidic buffers (ultrapure water or 0.1% TFA) and biological media (culture medium, physiological saline or plasma) at concentrations below 50 µM. Above this concentration, probe aggregation could be observed, especially in acidic buffers. To test the specificity of the enzymatic reaction, a control probe was synthetized using a modified peptide sequence where the L-Val was replaced by the antipodal D-Ala (Fig. 1).

Biochemical characterization of QCASP3.2

As determined by the increase of its fluorescence, QCASP3.2 was cleaved by recombinant human or murine caspase-3 but not by murine caspase-1, -8 and -11 or plasma (Fig. 2A). Moreover, probe activation was efficiently inhibited by the addition of Ac-DEVD-CHO, a

caspase-3 inhibitor (Fig. 2A). The incubation of the control probe with human or murine recombinant caspase-3 did not lead to any fluorescent emission (Fig. 2B).

The representation of the initial velocities (V_i) for each concentration of substrate followed a hyperbolic curve indicating that recombinant caspase-3 cleaves QCASP3.2 according to the Michaelis-Menten model (Fig. 2C). Using the double-inverse relation of Lineweaver-Burk, the kinetic parameters of QCASP3.2 cleavage were determined. The calculated Michaelis constant (K_M) was 9.35 ± 1.78 µM which reflects a high affinity between the enzyme and QCASP3.2. Furthermore, the catalytic turnover (k_{cat}) was 0.298 ± 0.035 s^{-1} which leads to a k_{cat}/K_M ratio of 31.8 × 10^3 $s^{-1}M^{-1}$.The final fluorescence intensity compared to the background signal strongly increased as probe concentration raised, to reach a maximum in the presence of 8 µM of QCASP3.2 (Fig. 2D). Finally, the V_i observed after cleavage of QCASP3.2 at either 1 or 5 µM in the presence of graded concentrations of human recombinant caspase-3 followed a linear relationship (Fig. 2E).

Cerebellar granule cells (CGC) as a model to investigate neuronal apoptosis

In the present study, cultured CGC were used as a model for the determination of caspase activity in neurons (Vaudry et al. 2000; 2003), to test and characterize QCASP3.2. Treatment of granule neurons with graded concentrations of H_2O_2 induced a dose-dependent increase of caspase-3 activity as measured with the Apo-ONE Caspase-3/7 Assay commercial kit (Fig. 3A). The maximum effect on caspase-3 activity (+ 73%) was observed in the presence of 40 µM H_2O_2 (Fig. 3A) and can be correlated with subsequent CGC death (Fig. 3B). Application of PACAP (100 nM) alone on cultured neurons only slightly reduced caspase-3 activity but a concomitant

administration of PACAP with H_2O_2 reversed the effect of both 20 and 40 µM H_2O_2 by decreasing caspase-3 activity of 31 and 33% respectively (Fig. 3C). Consequently, PACAP completely blocked the neurotoxic effect of both 20 and 40 µM H_2O_2 (Fig. 3D).

QCASP3.2 cleavage by neuronal lysates

Incubation of QCASP3.2 with a lysate from control CGC led to a rapid increase of near-infrared fluorescence signal, indicating the presence in the neurons of active enzymes able to cleave the probe (Fig. 4A). Pre-incubation of the cells with 20 µM Z-VAD-FMK, a general cell permeant caspase inhibitor, markedly reduced QCASP3.2 cleavage (Fig. 4A, B). Incubation of QCASP3.2 with a lysate from PACAP (100 nM)-treated cells significantly reduced the fluorescence signal (Fig. 4C). In contrast, incubation of QCASP3.2 with a lysate from H_2O_2 (40 µM)-treated cells provoked a 58% increase in the fluorescence intensity. Finally, incubation of QCASP3.2 with a lysate from cells that had been co-treated with H_2O_2 and PACAP did not modify cleavage of the probe (Fig. 4C). A direct effect of H_2O_2 on QCASP3.2 fluorescence was excluded as incubation of the probe with graded concentrations of H_2O_2 (20-400 µM) did not modify the fluorescent signal.

Five protease inhibitors were also tested in order to investigate which enzyme was responsible for cleavage of QCASP3.2 in cultured neuronal lysate (Fig. 4D). Z-VAD-FMK and Ac-DEVD-CHO, a reversible caspase-3 inhibitor, totally abolished the catalytic reaction at concentrations of 10^{-6} M and 10^{-8} M, respectively. The use of Ac-YVAD-CHO, a potent reversible caspase-1 inhibitor, decreased the velocity of the reaction but only at 10^{-5} M. In contrast, antipain and leupeptin, two serine protease inhibitors, had no effect.

QCASP3.2 cleavage by living cultured neurons

As the probe was designed for in vivo imaging, its potential toxicity and ability to enter the cells were tested. Exposure of cultured neurons to QCASP3.2 for 24 hours did not modify their survival either in control conditions or under H_2O_2 treatment (Fig. 5A). A 6-hour incubation of living neurons with QCASP3.2 provoked a gradual increase of the fluorescent signal. Treatment of cells for 6 hours with PACAP (100 nM) reduced by 25% the fluorescence intensity (Fig. 5B). In contrast, addition of H_2O_2 (40 µM) increased by 68% the fluorescence signal. Co-incubation with PACAP significantly attenuated the H_2O_2-induced fluorescence rise (Fig. 5B). Moreover, incubation of cells with Z-VAD-FMK reduced by more than 55% the cleavage rate of QCASP3.2 (Fig. 5C). The cleavage likely occurred inside the cells because conditioned supernatants only induced a very limited increase of the fluorescence intensity which was not affected by treatments (Control, PACAP, H_2O_2 or PACAP + H_2O_2). Microscopic observation of cultured neurons incubated with QCASP3.2 confirmed that the probe can enter into cells and revealed different labeling patterns. Healthy neurons with long extensions were only labeled with calcein (Fig. 6A), a sensor of viability, and did not exhibit any QCASP3.2 signal (Fig. 6B). Some round cells also revealed a green uniform staining (Fig. 6C), whereas others showed a patchy appearance with both calcein and QCASP3.2 labeling, indicating that although the cells were still viable they contained activated caspase-3 (Fig. 6D, E). These neurons also exhibited vacuolization which are characteristic of apoptotic cells (Fig. 6D, E). Finally, in our culture conditions, some cells, in a late apoptotic stage, were only labeled with QCASP3.2 (Fig. 6F). Quantification was performed by means of flow cytometry. Based on red and green fluorescence,

different populations were isolated. PACAP (100 nM) alone had no effect on the proportion of cleaved QCASP3.2-positive cells (Fig. 6G). Treatment with H_2O_2 (40 µM) provoked a 284% massive increase of the number of QCASP3.2-labeled neurons. Co-incubation with H_2O_2 and PACAP slightly reduced the number of QCASP3.2-positive cells but the difference was not statistically significant (Fig. 6G).

In vivo QCASP3.2 cleavage

In order to test the QCASP3.2 probe *in vivo*, we used a rodent model of permanent middle cerebral artery occlusion (MCAO), which led after 48 hours to a mean infarct volume of 20.2 ± 1.8 mm3. The lesion, corresponding to the unstained region of the brain, was located exclusively at the cortical level (Fig. 7A). Immunochemical labeling performed 24 hours after ischemia with an antibody directed against the cleaved form of caspase-3 revealed the presence of positive cells in the ischemic hemisphere (Fig. 7B). Intravenous injection of QCASP3.2, 24 hours after the focal ischemia (when caspase-3 was activated), led to a fluorescent signal detected in the right hemisphere of a brain tissue slice (Fig. 7D, G) while no fluorescence was recorded in the contralateral hemisphere of the mouse brain (Fig. 7C, F). High magnification observation showed that the fluorescence signal was associated with cell bodies and located mainly around nuclei (Fig. 7G). Several control experiments were conducted by injection of either a negative control probe, which cannot be cleaved by caspase-3 (Fig. 7E, H), or of vehicle alone (Fig. 7J, K). In these conditions, a very faint and diffuse fluorescent signal was detected at the level of the infarcted cerebral parenchyma, probably due to the presence of hemoglobin in the infarcted tissue (Saliba 2005). Nevertheless, at high magnification, no specific labeling associated to cell

bodies could be observed in these control animals (Fig. 7H, K). Finally, no fluorescent signal was detected in sham animals injected with the probe (Fig. 7I).

Discussion

Biochemical characterization of QCASP3.2

The protease-activable near infra-red fluorescent probe QCASP3.2 was engineered to be sensitive and specific of caspase-3 activity by using the peptide substrate Asp-Glu-Val-Asp (DEVD). Even though the DEVD tetrapeptide is recognized by both caspase 3 and -7 (Alnemri et al. 1996), it is established that caspase 3 is actively well expressed in the brain while caspase 7 is present at very low or undectable level in this tissue (Juan et al. 1997). Several recombinant caspases were tested to demonstrate the functionality of QCASP3.2, and as expected only murine and human caspase-3 could cleave the DEVD motif. Moreover, the replacement of the L-Val by the antipodal D-Ala in the control probe assessed the selectivity of caspase-3 for the DEVD motif entirely composed of L-amino acids.

Kinetic analyses revealed that QCASP3.2 is cleaved by recombinant human caspase-3 according a Michaelis-Menten model, suggesting that the two active sites of caspase-3 (Rotonda et al. 1996) act in an independent manner and do not cooperate. The calculated K_M for QCASP3.2 is consistent with previously published values (Nicholson et al. 1995), indicating that neither the cyanine 5.0 nor the quenching group affect the recognition of DEVD by recombinant caspase-3. It also reflects a high affinity between the enzyme and QCASP3.2. The catalytic turnover k_{cat} is below previous data obtained with other substrates containing the DEVD sequence. It should be

pointed out that the data available are very heterogeneous. For instance, a 16-fold difference has been reported, for the same substrate Ac-DEVD-amc, suggesting a predominant role of the experimental conditions in the determination of the k_{cat} value (Garcia-Calvo et al. 1999; Moretti et al. 2002). In order to have a validated comparison, we independently determined this value in a parallel experiment with Ac-DEVD-amc (k_{cat} = 0.75 s^{-1}) and QCASP3.2 (k_{cat} = 0.30 s^{-1}). The k_{cat}/K_M ratio is consistent with values reported for other protease substrates designed for *in vivo* imaging, indicating that QCASP3.2 could be a suitable probe for *in vivo* experiments (Zhang et al. 2009). Moreover, as the rate of the reaction is directly proportional to the concentration of recombinant caspase-3, QCASP3.2 represents a tool to quantify the amount of active enzyme.

QCASP3.2 cleavage in neurons is specific of caspase-3 activity

Caspase activation is an early event in the apoptotic process, which can be detected before cell death occurs (Davoli et al. 2002; Lakhani et al. 2006). In the present study, cultured CGC were used as a model for the determination of caspase activity in neurons (Vaudry et al. 2000; 2003), to test and characterize QCASP3.2. The occurrence of basal caspase-3 activity in lysates from CGC is consistent with the fact that, in these culture conditions, cells slowly die by apoptosis within 3 or 4 days (Gonzalez et al. 1997). Other proteases such as calpain (Ortega and Moran 2011) or caspase-1 (Tanaka et al. 1998) are also activated when CGC enter apoptosis. Inhibitors directed against several proteases ensured that QCASP3.2 cleavage in cerebellar neurons was specifically due to the presence of active caspase-3. Indeed, antipain and leupeptin had no effect on QCASP3.2 cleavage which demonstrated that cathepsin, plasmin, trypsin, papain and calpain, do not recognize the substrate. Z-VAD-FMK, a broad spectrum caspase inhibitor, significantly reduced the V_i which indicates the involvement of this family of proteases. The potent caspase-1

inhibitor, Ac-YVAD-CHO, could only decrease the velocity of the reaction at a concentration of 10^{-5} M whereas it inhibits caspase-1 activity with a K_i in the nanomolar range (Thornberry et al. 1994). In the present experiments, the most potent inhibitor of QCASP3.2 cleavage was Ac-DEVD-CHO which exhibited a K_i of 0.53 nM, a value close to that previously obtained with recombinant caspase-3 (Chen et al. 2006; Fang et al. 2006).

Effects of PACAP and H_2O_2 on caspase-3 activity and QCASP3.2 cleavage

Oxidative compounds are known to induce apoptotic cell death via the mitochondrial pathway and caspase-3 activation. At low concentrations, the effect of H_2O_2 on cell survival mirrored the dose-dependent increase of caspase-3 activity. At higher concentrations (80 µM and above) there was no correlation between caspase activation and cell death, probably because in these conditions, most cells die by necrosis (Aito et al. 2004). The neuropeptide pituitary adenylate cyclase-activating polypeptide (PACAP) can prevent apoptosis of CGC induced by reactive oxygen species by reducing caspase-3 activity (Vaudry et al. 2002). The robust neuroprotective effect of PACAP was also confirmed *in vivo* using various animal models of stroke (Ohtaki et al. 2006; Dejda et al. 2011; Lazarovici et al. 2012). In neuronal lysate and living CGC, QCASP3.2 was able to detect the deleterious effect of H_2O_2 and the protective activity of PACAP, indicating that this probe is adapted to determine caspase-3 enzymatic activity in cellular lysate as well as within cultured neurons. Caspase-3 can be released in late stage of apoptosis from cultured cells and retained a proteolytic activity (Hentze et al. 2001). As culture supernatants were not potent inducer of QCASP3.2 cleavage, it strongly suggests that QCASP3.2 can enter into the cells where it gets cleaved by endogenous enzymes.

QCASP3.2 allows visualization of caspase-3 activation

Confocal microscopic observation of cultured CGC revealed cells with well–developed extensions forming a network, and isolated, round and shrunken cells. This is in accordance with the fact that these cells are cultured in survival conditions leading to their natural progressive degeneration (Gonzalez et al., 1997). Incubation with QCASP3.2 demonstrated that its activation occurred specifically inside neurons with round morphology and allowed the discrimination of two kinds of apoptotic cells: viable neurons containing active caspase-3 that are just entering apoptosis, and dying cells that are in a late stage of apoptosis. The concomitant observation of different stages of apoptosis highlights the fact that cultured cells are heterogeneous and undergo cell death at different rates (Smolewski et al. 2002).

To translate the findings in vivo, a rodent stroke model was used. To monitor caspase-3 activity, the intravenous injection of QCASP3.2 was realized 24 hours after the insult when caspase-3 was found to be activated, which is consistent with previous reports (Zhu et al., 2004). A fluorescent signal was detected in cell bodies of the ischemic hemisphere. Interstitial fluorescence was also observed which could result in part from active caspase-3 released from dead cells (Hentze et al. 2001).

In conclusion, we have developed a Cy 5.0-labeled probe, QCASP3.2, to detect caspase-3 activity in living neurons. This probe is recognized with a high affinity and a high specificity by its target, and appears to be well suited to monitor the effects of anti-apoptotic drugs on caspase-

3 activity. Experiments conducted with mice revealed that QCASP3.2 can be activated in animals after stroke. One of the advantages of this probe is that it can be used for a wide spectrum of experiments ranging from cell lysates analysis to *in vivo* investigations. Moreover the wavelength of the fluorescent signal generated by QCASP3.2, in the near infra-red domain, enables in-depth travel of the light through tissues and should thus allow the monitoring of the signal in living animals with an optical imager.

Acknowledgments

The authors thank Drs. M. Bénard and L. Galas, from the Cell Imaging Platform of Normandy (PRIMACEN) for excellent technical assistance in microscopy experiments, and Dr. N. Thorel for her contribution to cytometry experiments.

References

Aito H., Aalto K. T. and Raivio K. O. (2004) Adenine nucleotide metabolism and cell fate after oxidant exposure of rat cortical neurons: effects of inhibition of poly(ADP-ribose) polymerase. Brain Res. 1013, 117–124.

Alnemri E. S., Livingston D. J., Nicholson D. W., et al. (1996) Human ICE/CED-3 protease nomenclature. Cell 87, 171.

Bullok K. and Piwnica-Worms D. (2005) Synthesis and characterization of a small, membrane-permeant, caspase-activatable far-red fluorescent peptide for imaging apoptosis. J. Med. Chem. 48, 5404–5407.

Bullok K. E., Maxwell D., Kesarwala A. H., et al. (2007) Biochemical and in vivo characterization of a small, membrane-permeant, caspase-activatable far-red fluorescent peptide for imaging apoptosis. Biochemistry 46, 4055–4065.

Chen Y. H., Zhang Y. H., Zhang H. J., et al. (2006) Design, synthesis, and biological evaluation of isoquinoline-1,3,4-trione derivatives as potent caspase-3 inhibitors. J. Med. Chem. 49, 1613–1623.

Cortez-Retamozo V., Swirski F. K., Waterman P., et al. (2008) Real-time assessment of inflammation and treatment response in a mouse model of allergic airway inflammation. J. Clin. Invest. 118, 4058–4066.

Davoli M. A., Fourtounis J., Tam J., et al. (2002) Immunohistochemical and biochemical assessment of caspase-3 activation and DNA fragmentation following transient focal ischemia in the rat. Neuroscience 115, 125–136.

Dejda A., Seaborn T., Bourgault S., et al. (2011) PACAP and a novel stable analog protect rat brain from ischemia: Insight into the mechanisms of action. Peptides 32, 1207–16.

Elmore S. (2007) Apoptosis: a review of programmed cell death. Toxicol. Pathol. 35, 495–516.

Fang B., Boross P. I., Tozser J. and Weber I. T. (2006) Structural and kinetic analysis of caspase-3 reveals role for s5 binding site in substrate recognition. J. Mol. Biol. 360, 654–666.

Garcia-Calvo M., Peterson E. P., Rasper D. M., et al. (1999) Purification and catalytic properties of human caspase family members. Cell Death Differ. 6, 362–369.

Gonzalez B. J., Basille M., Vaudry D., Fournier A. and Vaudry H. (1997) Pituitary adenylate cyclase-activating polypeptide promotes cell survival and neurite outgrowth in rat cerebellar neuroblasts. Neuroscience 78, 419–430.

Hengartner M. O. (2000) The biochemistry of apoptosis. Nature 407, 770–776.

Hentze H., Schwoebel F., Lund S., et al. (2001) In vivo and in vitro evidence for extracellular caspase activity released from apoptotic cells. Biochem. Biophys. Res. Commun. 283, 1111–1117.

Jacobson M. D., Weil M. and Raff M. C. (1997) Programmed cell death in animal development. Cell 88, 347–354.

Juan T. S., McNiece I. K., Argento J. M., et al. (1997) Identification and mapping of Casp7, a cysteine protease resembling CPP32 beta, interleukin-1 beta converting enzyme, and CED-3. Genomics 40, 86–93.

Kume T., Taguchi R., Katsuki H., et al. (2006) Serofendic acid, a neuroprotective substance derived from fetal calf serum, inhibits mitochondrial membrane depolarization and caspase-3 activation. Eur. J. Pharmacol. 542, 69–76.

Lakhani S. A., Masud A., Kuida K., et al. (2006) Caspases 3 and 7: key mediators of mitochondrial events of apoptosis. Science 311, 847–851.

Lapeyre M., Leprince J., Massonneau M., et al. (2006) Aryldithioethyloxycarbonyl (Ardec): a new family of amine protecting groups removable under mild reducing conditions and their applications to peptide synthesis. Chemistry 12, 3655–3671.

Lazarovici P., Cohen G., Arien-Zakay H., et al. (2012) Multimodal neuroprotection induced by PACAP38 in oxygen-glucose deprivation and middle cerebral artery occlusion stroke models. J. Mol. Neurosci. 48, 526–40.

Lin T. N., He Y. Y., Wu G., Khan M. and Hsu C. Y. (1993) Effect of brain edema on infarct volume in a focal cerebral ischemia model in rats. Stroke 24, 117–21.

Liu H., Chang D. W. and Yang X. (2005) Interdimer processing and linearity of procaspase-3 activation. A unifying mechanism for the activation of initiator and effector caspases. J. Biol. Chem. 280, 11578–11582.

Liu Y., Kati W., Chen C. M., Tripathi R., Molla A. and Kohlbrenner W. (1999) Use of a fluorescence plate reader for measuring kinetic parameters with inner filter effect correction, Anal. Biochem. 267, 331–335.

Lloyd-Jones D., Adams R., Carnethon M., et al. (2009) Heart disease and stroke statistics--2009 update: a report from the American Heart Association Statistics Committee and Stroke Statistics Subcommittee. Circulation 119, 480–486.

Love S., Barber R., Srinivasan A. and Wilcock G. K. (2000) Activation of caspase-3 in permanent and transient brain ischaemia in man. Neuroreport 11, 2495–2499.

Moretti A., Weig H. J., Ott T., et al. (2002) Essential myosin light chain as a target for caspase-3 in failing myocardium. Proc. Natl. Acad. Sci. USA 99, 11860–11865.

Nicholson D. W., Ali A., Thornberry N. A., et al. (1995) Identification and inhibition of the ICE/CED-3 protease necessary for mammalian apoptosis. Nature 376, 37–43.

Ohtaki H., Nakamachi T., Dohi K., et al. (2006) Pituitary adenylate cyclase-activating polypeptide (PACAP) decreases ischemic neuronal cell death in association with IL-6. Proc. Natl. Acad. Sci. USA 103:7488–93.

Ortega A. and Moran J. (2011) Role of cytoskeleton proteins in the morphological changes during apoptotic cell death of cerebellar granule neurons. Neurochem Res. 36, 93–102.

Pantos C., Mourouzis I., Saranteas T., et al. (2009) Thyroid hormone improves postischaemic recovery of function while limiting apoptosis: a new therapeutic approach to support hemodynamics in the setting of ischaemia-reperfusion? Basic Res. Cardiol. 104, 69–77.

Petrovsky A., Schellenberger E., Josephson L., Weissleder R. and Bogdanov A. Jr. (2003) Near-infrared fluorescent imaging of tumor apoptosis. Cancer Res. 63, 1936–1942.

Raymond S. B., Skoch J., Hills I. D., Nesterov E. E., Swager T. M. and Bacskai B. J. (2008) Smart optical probes for near-infrared fluorescence imaging of Alzheimer's disease pathology. Eur. J. Nucl. Med. Mol. Imaging 35 Suppl 1, S93–98.

Rotonda J., Nicholson D. W., Fazil K. M., et al. (1996) The three-dimensional structure of apopain/CPP32, a key mediator of apoptosis. Nat. Struct. Biol. 3, 619–625.

Saliba E. (2005) Non-invasive techniques to investigate the newborn brain. Arch. Pediatr. 12, 737–740.

Smolewski P., Grabarek J., Halicka H. D. and Darzynkiewicz Z. (2002) Assay of caspase activation in situ combined with probing plasma membrane integrity to detect three distinct stages of apoptosis. J. Immunol. Methods 265, 111–21.

Stennicke H. R. and Salvesen G. S. (1997) Biochemical characteristics of caspases-3, -6, -7, and -8. J. Biol. Chem. 272, 25719–25723.

Takadera T., Fujibayashi M., Kaniyu H., Sakota N. and Ohyashiki T. (2007) Caspase-dependent apoptosis induced by thapsigargin was prevented by glycogen synthase kinase-3 inhibitors in cultured rat cortical neurons. Neurochem. Res. 32, 1336–1342.

Tanaka M., Sawada M., Miura M. and Marunouchi T. (1998) Insulin-like growth factor-I analogue prevents apoptosis mediated through an interleukin-1 beta converting enzyme (caspase-1)-like protease of cerebellar external granular layer neurons: developmental stage-specific mechanisms of neuronal cell death. Neuroscience 84, 89–100.

Thornberry N. A., Peterson E. P., Zhao J. J., Howard A. D., Griffin P. R. and Chapman K. T. (1994) Inactivation of interleukin-1 beta converting enzyme by peptide (acyloxy)methyl ketones. Biochemistry 33, 3934–3940.

Vaudry D., Falluel-Morel A., Bourgault S., et al. (2009) Pituitary adenylate cyclase-activating polypeptide and its receptors: 20 years after the discovery. Pharmacol. Rev. 61, 283–357.

Vaudry D., Falluel-Morel A., Leuillet S., Vaudry H. and Gonzalez B. J. (2003) Regulators of cerebellar granule cell development act through specific signaling pathways. Science 300, 1532–1534.

Vaudry D., Gonzalez B. J., Basille M., et al. (2000) The neuroprotective effect of pituitary adenylate cyclase-activating polypeptide on cerebellar granule cells is mediated through inhibition of the CED3-related cysteine protease caspase-3/CPP32. Proc. Natl. Acad. Sci. USA 97, 13390–13395.

Vaudry D., Pamantung T. F., Basille M., et al. (2002) PACAP protects cerebellar granule neurons against oxidative stress-induced apoptosis. Eur. J. Neurosci. 15, 1451–1460.

Weissleder R. and Ntziachristos V. (2003) Shedding light onto live molecular targets. Nat. Med. 9, 123–128.

Weissleder R. and Pittet M. J. (2008) Imaging in the era of molecular oncology. Nature 452, 580–589.

Zhang Z., Fan J., Cheney P. P., et al. (2009) Activatable molecular systems using homologous near-infrared fluorescent probes for monitoring enzyme activities in vitro, in cellulo, and in vivo. Mol. Pharm. 6, 416–427.

Zheng Z., Zhao H., Steinberg G. K. and Yenari M. A. (2003) Cellular and molecular events underlying ischemia-induced neuronal apoptosis. Drug News Perspect. 16, 497–503.

Zhu S., Li M., Figueroa B. E., et al. (2004) Prophylactic creatine administration mediates neuroprotection in cerebral ischemia in mice. J. Neurosci. 24, 5909–5912.

Legends to figures

Figure 1 Schematic structure of the far-red fluorogenic caspase-3 probe QCASP3.2 and the control probe. The two probes are composed of a peptidic backbone grafted at the N-terminal side with Cy5.0 and at the C-terminal side with the quenching group QSY®21.

Figure 2 Biochemical characterization of QCASP3.2. (A) Typical time-course effect of caspases and plasma on far-red QCASP3.2 probe fluorescence emission. QCASP3.2 (1 µM) was incubated in the presence of recombinant murine caspase-1, -3, -8 or -11 and human caspase-3 or -7 in caspase assay buffer. Caspases-3 were pre-incubated or not with Ac-DEVD-CHO (0.25 µM). The fluorescence signal was monitored over time with excitation at 645 nm and emission at 670 nm. (B) Typical time-course effect of caspases-3 and plasma on fluorescence emission of QCASP3.2 and the control probe containing the antipodal D-Ala. (C) Michaelis-Menten representation of the initial velocities (V_i) corrected for the inner-filter effect corresponding to each QCASP3.2 concentration used. Inset: Lineweaver-Burk representation; the intersection of the straight line and the abscissa axis equals $-1/K_M$. (D) Signal / background fluorescence ratio of QCASP3.2 determined at the end of the catalytic reaction. (E) Linearity of QCASP3.2 cleavage by graded concentrations of recombinant human caspase-3.

Figure 3 Induction of apoptosis in cerebellar granule cells. (A, B) Effect of graded concentrations of H_2O_2 on caspase-3 activity and cell survival. (C, D) Effect of PACAP (100 nM) on H_2O_2-induced caspase-3 activation and cell death. Caspase-3 activity (A, C) and cultured granule cell viability (B, D) were determined 6 and 24 hours after the beginning of the treatment,

respectively. Results are expressed as percentage of control. Each value is the mean ± SEM of at least three independent experiments performed in triplicate. * $p<0.05$; ** $p<0.01$; *** $p<0.001$ vs control; § $p<0.05$; §§ $p<0.01$ vs H_2O_2 (Kruskal-Wallis test followed by Mann and Whitney test).

Figure 4 Cleavage of the QCASP3.2 probe by neuronal lysates. (A) Time-course of QCASP3.2 cleavage with neuronal lysates. (B, C) Effect of pre-incubation of cells with (B) Z-VAD-FMK and (C) PACAP and/or H_2O_2 on initial velocities (V_i) of QCASP3.2 cleavage by neuronal lysates. (D) Effect of increasing concentrations of protease inhibitors (Ac-DEVD-CHO, Ac-YVAD-CHO, Z-VAD-FMK, antipain and leupeptin) on V_i of QCASP3.2 cleavage in neuronal lysate. Each value is the mean ± SEM of at least three independent experiments performed in triplicates. * $p<0.05$ vs control; § $p<0.05$ vs H_2O_2 (Kruskal-Wallis test followed by Mann and Whitney test).

Figure 5 Cleavage of the QCASP3.2 probe in living neurons. (A) Effect of incubation with QCASP3.2 (5 µM) in the absence or presence of H_2O_2 (40 µM) on survival of cultured cerebellar granule cells. (B) Effect of PACAP (100 nM) and/or H_2O_2 (40 µM) or (C) the pan-caspase inhibitor Z-VAD-FMK (20 µM) on QCASP3.2 cleavage in cultured cerebellar granule cells. Each value is the mean ± SEM of at least three independent experiments performed in triplicates. * $p<0.05$; ** $p<0.01$; *** $p<0.001$ vs control; § $p<0.05$ vs H_2O_2 (Kruskal-Wallis test followed by Mann and Whitney test).

Figure 6 Microscopic observation of neurons incubated with QCASP3.2. (A-F) Visualization of cerebellar granule neurons stained in green with calcein and in red with activated QCASP3.2.

(A) Granule neurons cultured for 24 hours in serum-free conditions exhibit mixed phenotypes with healthy cells (green) and dying cells (red). High magnification of a healthy neuron with extension (B), of a round healthy neuron (C, F, green cell), and of apoptotic neurons in early (D, E) or late stage (F, red cell). Scale bar = 30 µm (A), 5 µm (B-F). (G) Cytometric analysis of neurons incubated with QCASP3.2. Each value is the mean ± SEM of at least three independent experiments. * $p<0.05$ vs control (Kruskal-Wallis test followed by Mann and Whitney test).

Figure 7 Imaging of the brain infarct area with QCASP3.2 after permanent focal cerebral ischemia in the mouse. (A) Thionine staining of a brain tissue slice 48 hours after permanent MCAO allows detection of the uncolored infarct area. Rectangles correspond to region observed by fluorescence microscopy and illustrated in B-K. (B) Activated caspase-3 is detected after stroke in the ipsilateral hemisphere. After an intravenous injection of QCASP3.2, no signal was recorded in the contralateral hemisphere (C, F) whereas a red fluorescence was observed in the infarct area (D, G). No specific fluorescent signal was detected after the injection of the control probe (E, H), or the vehicle (J, K) and neither in sham operated mice injected with QCASP3.2 (I). Nuclei were stained with DAPI (blue). Cx, cortex; St, striatum. Scale bar = 1 mm (A), 500 µm (B-E, I, J), 50 µm (F-H, K).

Figure
Click here to download Figure: Jolivel_figures.ppt

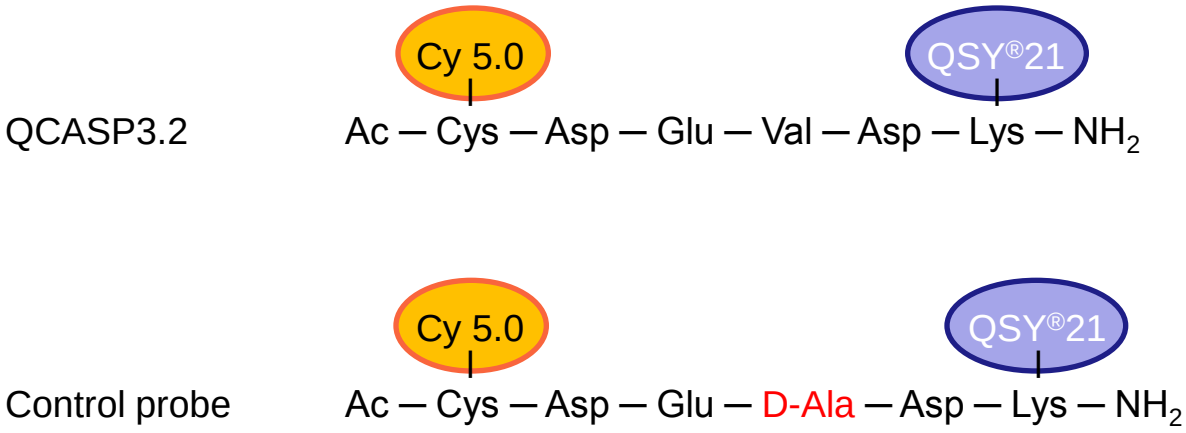

Figure 1

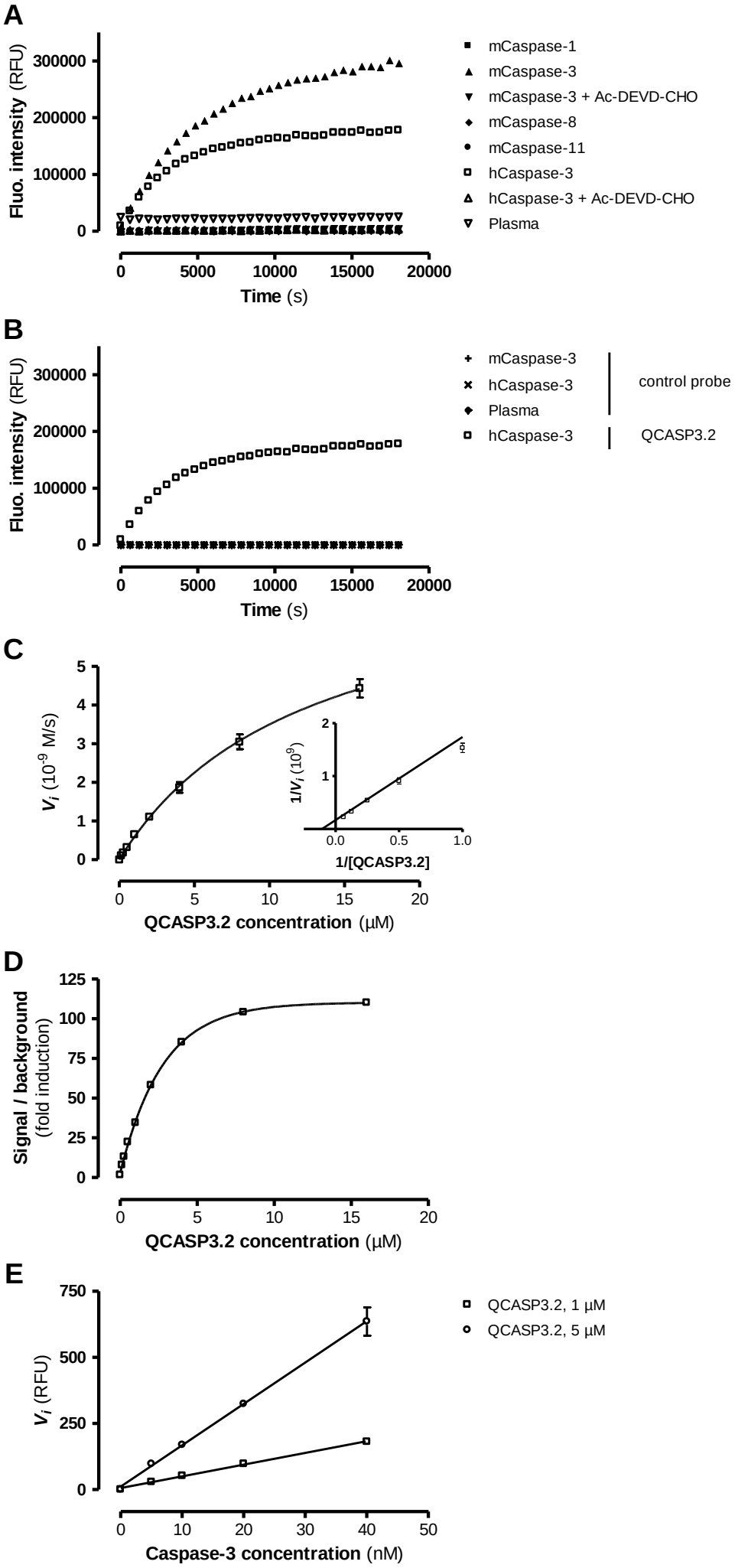
A
Fluo. intensity (RFU)
300000
200000
100000
0
0
5000
10000
15000
20000
Time (s)
mCaspase-1
mCaspase-3
mCaspase-3 + Ac-DEVD-CHO
mCaspase-8
mCaspase-11
hCaspase-3
hCaspase-3 + Ac-DEVD-CHO
Plasma
B
Fluo. intensity (RFU)
300000
200000
100000
0
0
5000
10000
15000
20000
Time (s)
mCaspase-3
hCaspase-3
Plasma
control probe
hCaspase-3
QCASP3.2
C
V_i (10^{-9} M/s)
5
4
3
2
1
0
0
5
10
15
20
QCASP3.2 concentration (µM)
$1/V_i$ (10^9)
2
1
0.0
0.5
1.0
1/[QCASP3.2]
D
Signal / background
(fold induction)
125
100
75
50
25
0
0
5
10
15
20
QCASP3.2 concentration (µM)
E
V_i (RFU)
750
500
250
0
0
10
20
30
40
50
Caspase-3 concentration (nM)
QCASP3.2, 1 µM
QCASP3.2, 5 µM

Figure 2

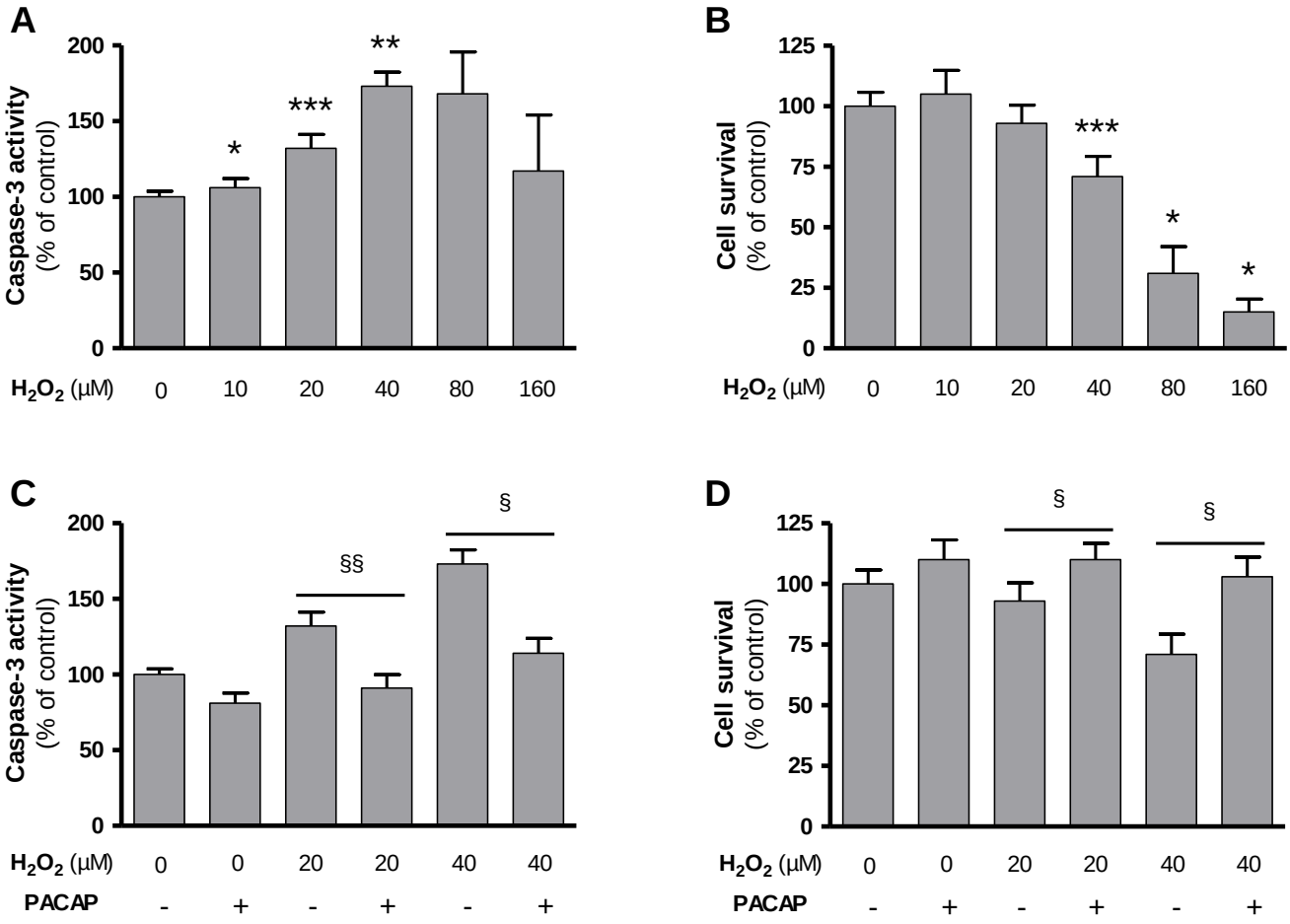
A
Caspase-3 activity
(% of control)
200
150
100
50
0
*
***
**
H2O2 (μM) 0 10 20 40 80 160
B
Cell survival
(% of control)
125
100
75
50
25
0
***
*
*
H2O2 (μM) 0 10 20 40 80 160
C
Caspase-3 activity
(% of control)
200
150
100
50
0
§§
§
H2O2 (μM) 0 0 20 20 40 40
PACAP - + - + - +
D
Cell survival
(% of control)
125
100
75
50
25
0
§
§
H2O2 (μM) 0 0 20 20 40 40
PACAP - + - + - +

Figure 3

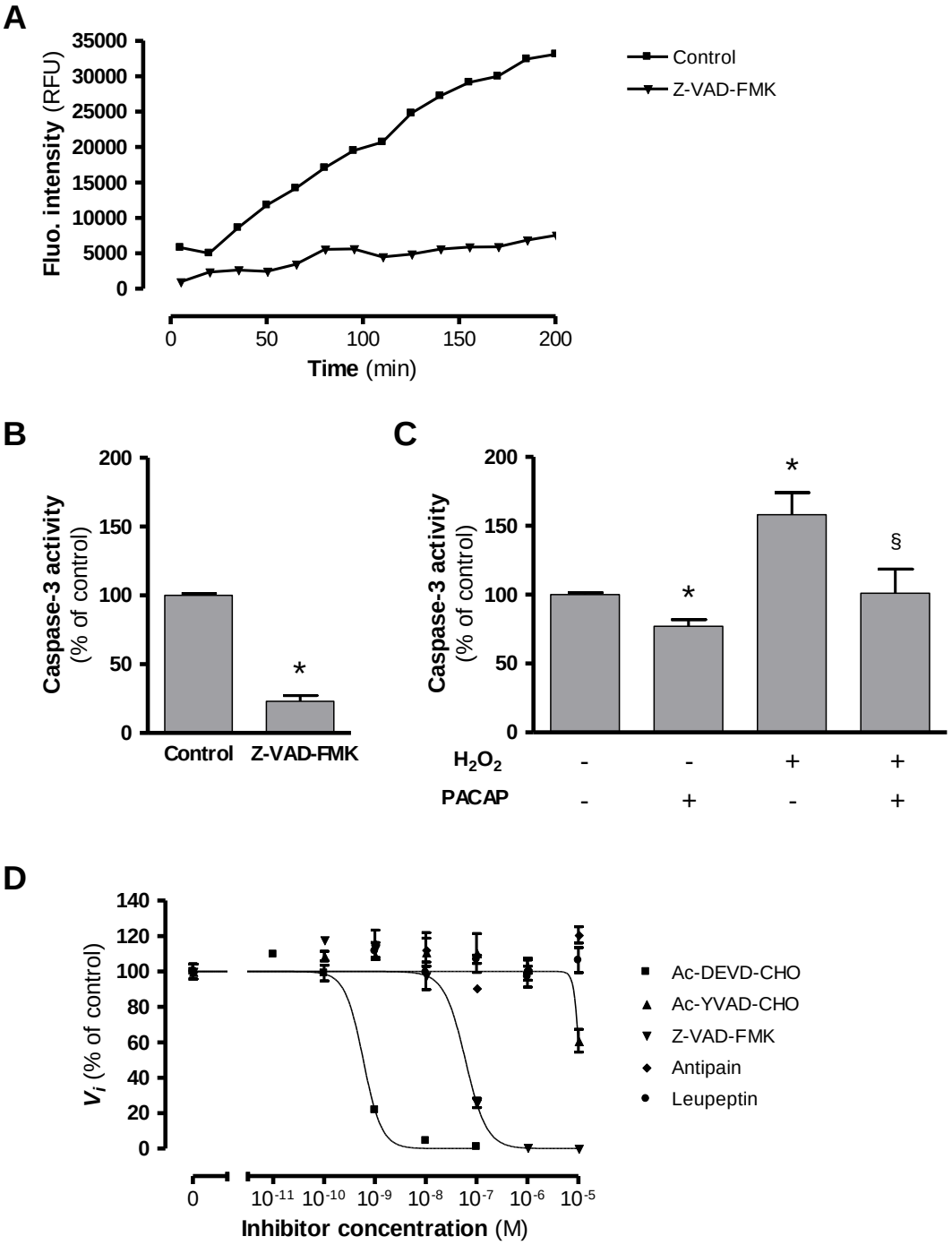
A
Fluo. intensity (RFU)
35000
30000
25000
20000
15000
10000
5000
0
0
50
100
150
200
Time (min)
Control
Z-VAD-FMK
B
Caspase-3 activity
(% of control)
200
150
100
50
0
*
Control
Z-VAD-FMK
C
Caspase-3 activity
(% of control)
200
150
100
50
0
*
*
§
H2O2 - - + +
PACAP - + - +
D
Vi (% of control)
140
120
100
80
60
40
20
0
0
10-11 10-10 10-9 10-8 10-7 10-6 10-5
Inhibitor concentration (M)
Ac-DEVD-CHO
Ac-YVAD-CHO
Z-VAD-FMK
Antipain
Leupeptin

Figure 4

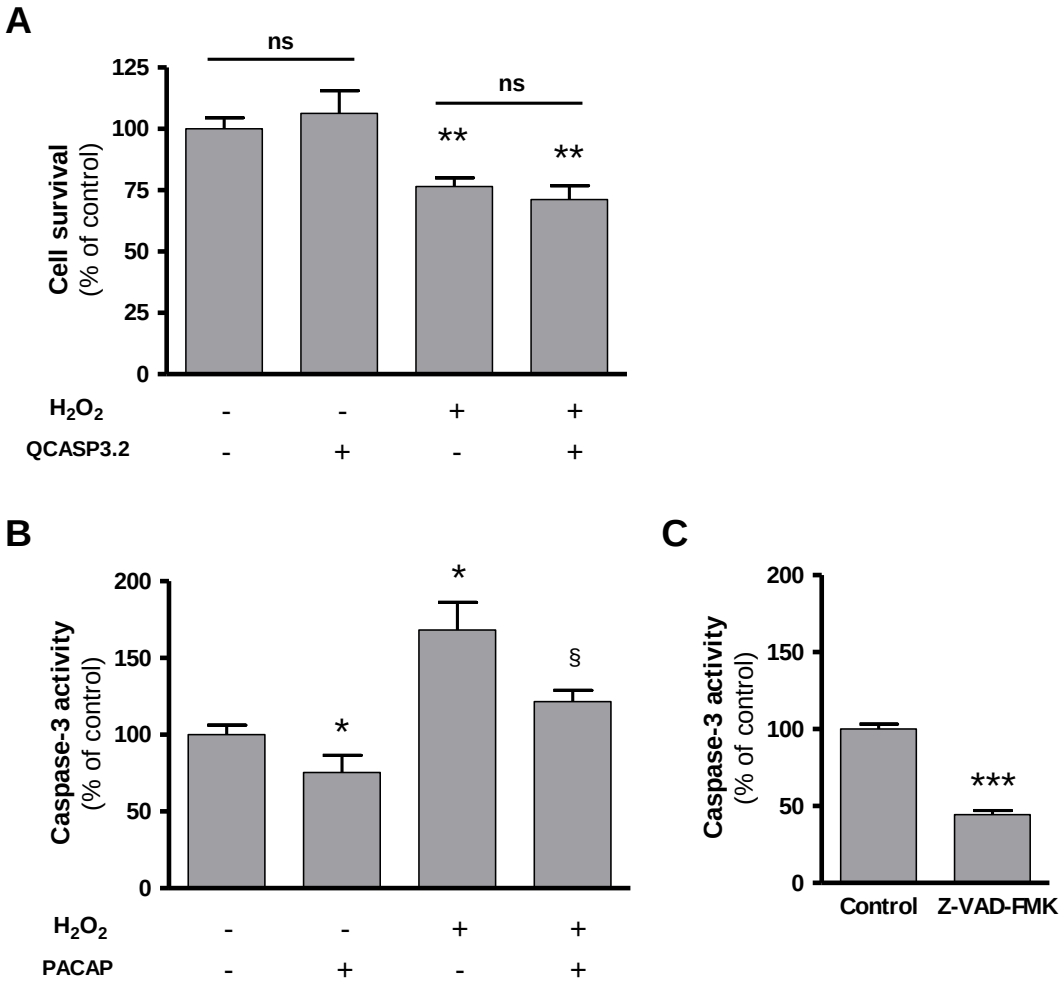
A
ns
ns
**
**
125
100
75
50
25
0
Cell survival
(% of control)
H2O2 - - + +
QCASP3.2 - + - +
B
*
*
§
200
150
100
50
0
Caspase-3 activity
(% of control)
H2O2 - - + +
PACAP - + - +
C
***
200
150
100
50
0
Caspase-3 activity
(% of control)
Control
Z-VAD-FMK

Figure 5

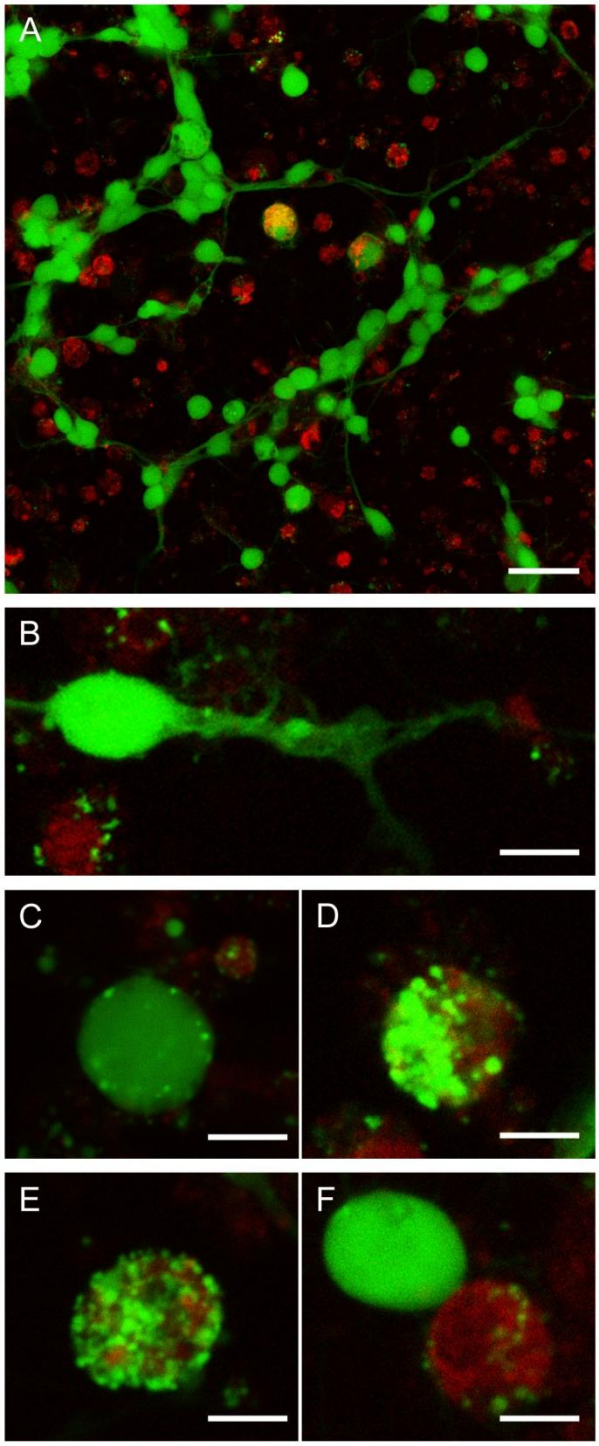
A
B
C
D
E
F

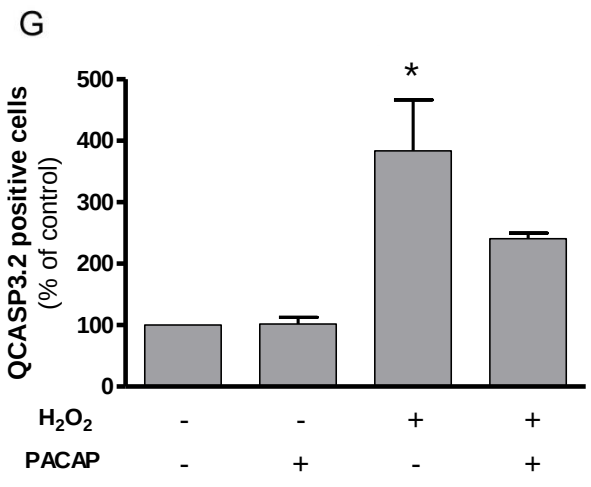
G
QCASP3.2 positive cells
(% of control)
500
400
300
200
100
0
*
H2O2 - - + +
PACAP - + - +

Figure 6

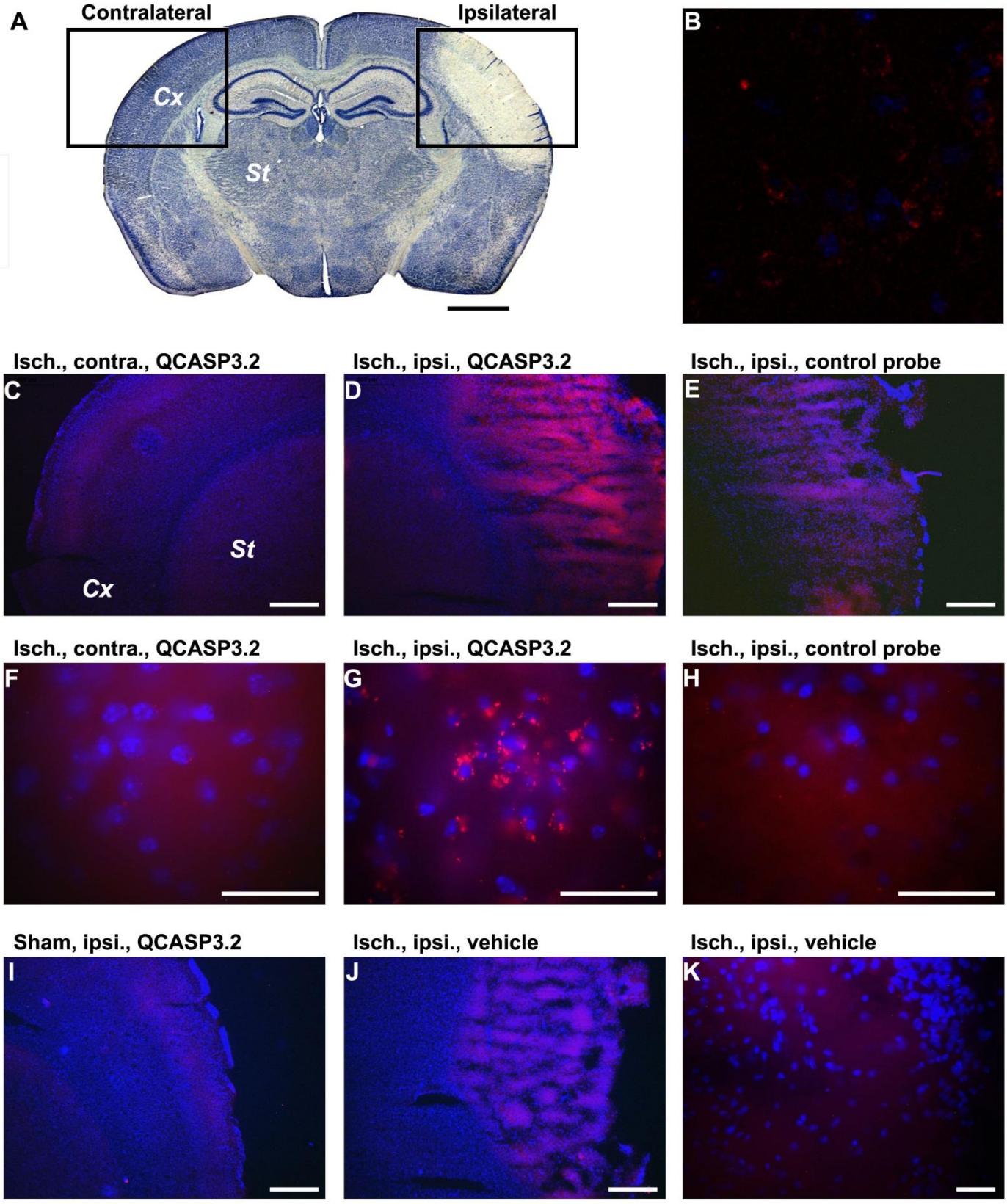
A
Contralateral
Ipsilateral
Cx
St
B
Isch., contra., QCASP3.2
Isch., ipsi., QCASP3.2
Isch., ipsi., control probe
C
St
Cx
D
E
Isch., contra., QCASP3.2
Isch., ipsi., QCASP3.2
Isch., ipsi., control probe
F
G
H
Sham, ipsi., QCASP3.2
Isch., ipsi., vehicle
Isch., ipsi., vehicle
I
J
K

Figure 7